Hexagonal Order in Crystalline and Columnar Phases of Hard Rods

Eric Grelet*

Centre de Recherche Paul Pascal, CNRS-Université Bordeaux 1, 115 Avenue Schweitzer, 33600 Pessac, France

(Received 14 December 2007; published 24 April 2008)

We report a study of colloidal suspensions of highly monodisperse semiflexible chiral rodlike viruses, denoted fd, in the range of high concentrations. Small angle x-ray scattering experiments reveal the existence of two hexagonal phases: the first one is crystalline and the second one is hexatic columnar, as shown by its short-range positional order. The suspension of rodlike viruses is the first experimental system showing the whole phase sequence with increasing particle concentration theoretically predicted for systems of hard rods, ranging from the chiral nematic via the smectic to columnar and crystalline phases.

DOI: 10.1103/PhysRevLett.100.168301 PACS numbers: 82.70.Dd, 61.05.C−, 61.30.−v

The entropy driven phase transition of suspensions of hard rods has been a subject of intensive theoretical [1] and experimental [2,3] investigations. Inspired by Onsager's work showing that a system of long thin particles interacting only by hard core repulsion can exhibit nematic ordering if the density is sufficiently high [4], computer simulation studies gave the first indication that excluded volume interactions alone could additionally account for the existence of more complex phases: smectic, columnar, and crystalline phases (Fig. 1) [5]. Recently, the whole phase diagram of rigid hard rods, including size polydispersity, has been predicted. Essentially, two parameters are needed to describe the system, namely, the density or volume fraction ϕ and the rod aspect ratio L/D [6]. However, suitable experimental systems for comparison and test of theoretical predictions are rare. For that purpose, the filamentous bacteriophage fd, which is a micron-length ($L = 0.88$ μm) semiflexible polyelectrolyte with a diameter of $D = 66$ Å and a persistence length of about $3L$, has been playing a major role [3]: due to their biological origin [7], fd viruses are highly monodisperse particles, whose interactions are predominantly repulsive. This monodispersity makes them a model system for studying the self-organization in complex fluids composed of rodlike particles. Up to now, experimental studies have been mainly focused on diluted fd suspensions with a typical volume fraction of rods $\phi < 0.2$: the existence of the isotropic, chiral nematic (or cholesteric) [8], and smectic [9] phases has been observed in solutions on increasing rod concentration. The existence of a smectic phase is an experimental evidence of the high monodispersity and therefore of the suitability of such filamentous viruses as model system [6]. In this Letter, the regime of high rod densities ($\phi > 0.2$) is investigated, and two phases with a sixfold symmetry are reported: a hexatic columnar phase with a two-dimensional hexagonal short-range translational order, and a crystalline phase of viruses where positional correlations are long-ranged in the three dimensions.

In order to study the structure of the liquid crystalline suspensions of filamentous viruses, small angle x-ray scattering (SAXS) has been performed. The range of investigated scattering vectors q corresponds to an interaxial spacing between two viruses of about one rod diameter. Figure 2(a) presents the typical diffraction pattern of an *oriented* sample (with the x-ray beam parallel to the virus long axis) at a volume fraction above the smectic range. This pattern exhibits a sixfold symmetry and displays many Bragg peaks, whose positions in reciprocal space relative to the position of the first peak are $1{:}\sqrt{3}{:}\sqrt{4}$ [Fig. 2(b)] characterizing a hexagonal positional order in the plane normal to the rods [10]. In combination with the lack of layered structure, i.e., of positional correlations along the viruses, evidenced by differential interference contrast (DIC) microscopy [Fig. 3(a)], this defines a *columnar phase* as depicted in Fig. 1. In such a mesophase, the rodlike viruses are confined to liquidlike columns which, in turn, are organized in a 2D hexagonal array. Moreover, the stripe texture seen in Fig. 2(d) originating from column undulations [11], is usually observed in columnar liquid crystals, both in the lyotropic columnar phase of DNA [12] and in thermotropic discotic mesophases [13]. The phase coexistence shown in Fig. 3(a) is

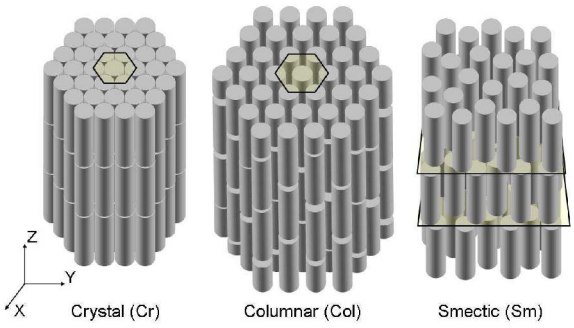

FIG. 1 (color online). Schematic representation of the crystal (Cr), columnar (Col), and smectic (Sm) phases of rodlike particles.

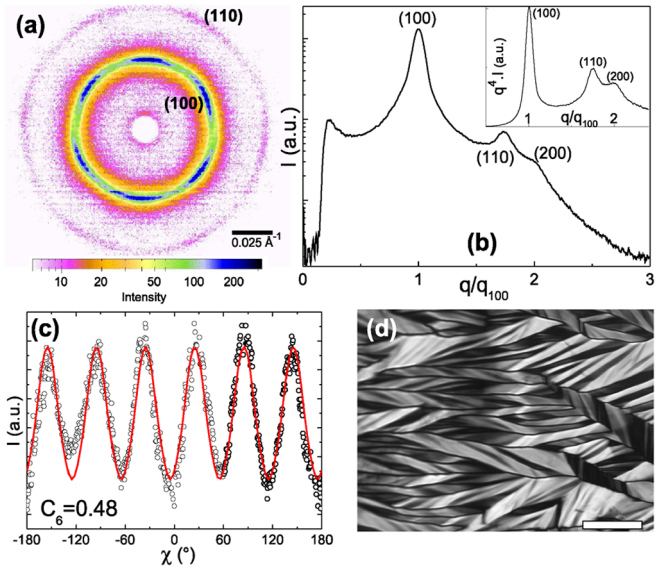

FIG. 2 (color online). (a) X-ray scattering pattern of the columnar monodomain exhibiting a sixfold symmetry and (b) its averaged radial profile showing the (100), (110), and (200) Bragg reflections [21] as the typical signature of a hexagonal packing [10]. Inset in (b): Porod representation of the scattered intensity for a better visualization of the different Bragg peaks. (c) From the sixfold azimuthal intensity modulation (open circles) is extracted the orientational order parameter, C_6, by a fit (red solid line) according to Eq. (1). (d) Optical texture of the columnar phase observed by polarizing microscopy. The scale bar indicates 30 μm.

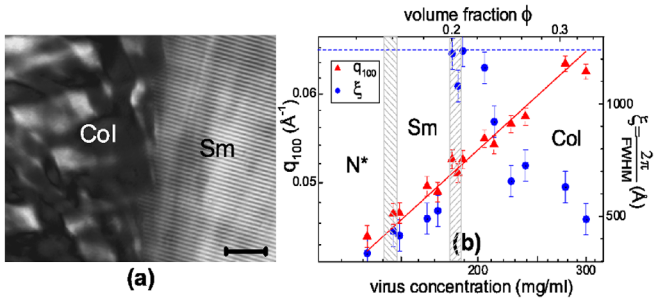

FIG. 3 (color online). (a) Coexistence of the columnar (left) and smectic (right) phases observed by DIC microscopy (digitally enhanced picture). The scale bar indicates 10 μm. (b) Log-log scale representation of the virus concentration (or the corresponding volume fraction ϕ) dependence of the (100) Bragg peak position (red triangles, $I = 50$ mM [7]). The red solid line is a data fit $q_{100} \propto \phi^{1/2}$, characterizing a swelling law of 2D order. Blue circles show the corresponding correlation length ξ and the blue dashed line indicates the instrumental resolution [21]. The phase coexistence ranges are shown by dashed regions.

the hallmark of a first order transition between a columnar and a smectic phase, which is reversible by dilution or concentration of the sample. If the particle size dispersity has been invoked in the appearance of a columnar phase [5,6], the rod flexibility of the fd virus has to play a significant role in the stabilization of the columnar ordering [14].

Surprisingly, the radial profile of the diffraction peaks shows substantial tails [Figs. 2(b) and 4(a)] and broadens beyond the instrumental resolution [Fig. 3(b)] with the disappearance of high order Bragg reflections. This indicates that short-range positional ordering takes place, which suggests a *hexatic* order. The hexatic structure, which was first proposed as an intermediate state in the scenario of two-dimensional melting [15], is defined by long-range sixfold orientational order while translational order is short-ranged by the introduction of topological defects [16]. The occurrence of dislocations destroys the long-range positional order but not the bond orientational order which stays long-ranged: a hexatic phase is expected with increasing concentration to display a decrease of the translational correlation length ξ, which is related to the density of defects [17,18]. This feature is experimentally observed in the concentration range of the columnar phase, as shown in Fig. 3(b).

In combination with the range of positional correlations, bond orientational order has been quantitatively measured on the arched Bragg reflections of the columnar monodomain [Fig. 2(a)]. Indeed, their large azimuthal width is an intrinsic feature of the hexatic order [19]. The angular dependence of the sixfold symmetric scattering function of the (100) reflection [Fig. 2(c)] has been Fourier analyzed [20]:

$$I(\chi) = I_0\left\{\frac{1}{2} + \sum_{n=1}^{\infty} C_{6n}\cos[6n(\chi - \chi_0)]\right\} + I_{BG}, \qquad (1)$$

where I_{BG} accounts for the background intensity and the coefficients C_{6n} measure the amount of $6n$-fold ordering. The fit yields $C_6 = 0.48$, $C_{12} = 0.03$, $C_{18} \approx C_{24} \approx \ldots \approx 0$, that denotes the existence of a significant long-range sixfold orientational order in the columnar phase, consistent with a hexatic structure [16]. Furthermore, the range of the orientational order correlations extends over macroscopic distances, that correspond at least to the sample area of the single domain covered by the x-ray beam [21].

A line shape analysis of the (100) Bragg peaks has been performed due to the specific profile expected in the hexatic phase (Fig. 4) [22]. For that purpose, an x-ray beam with high resolution, as obtained by synchrotron radiation, has to be used [23]. In a conventional liquid the positional correlations decay exponentially with distance, giving a Lorentzian scattering profile. The suppression of long-range translational order causes power-law singularities instead of delta-function-type diffraction peaks for an infinite crystal [16]. In the case of hexatic order, a square-root Lorentzian (SRL) profile is predicted because of the coupling between the bond orientational and the positional orders [22], that has been widely used experimentally [19]. The SRL distribution accounts for the existence of the

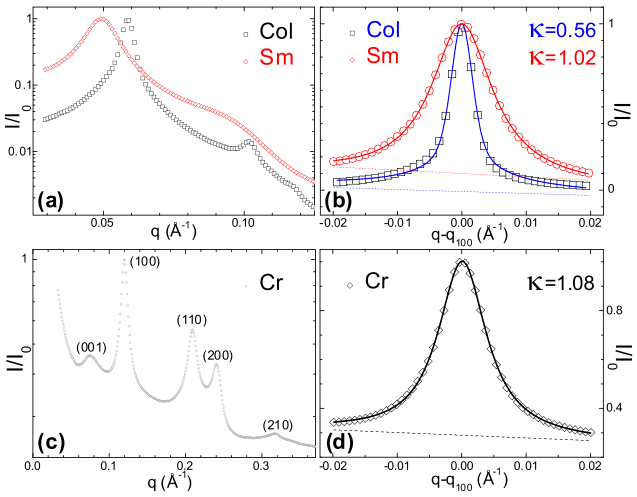

FIG. 4 (color online). Average radial intensity profile of the synchrotron SAXS patterns in the (a) smectic, columnar, and (c) crystalline phases [23]. (b),(d) Fits (solid lines) according to Eq. (2) of the (100) Bragg reflections (open symbols) which are not resolution limited. The dashed line shows the subtracted linear background.

diffuse scattering in the tails of the Bragg peaks, that leads to the attenuation of high order Bragg reflections. The shape of the (100) diffraction peak has therefore been fitted using a Pearson type VII function [25] with the exponent κ as a free parameter:

$$I(q) = \frac{I_0}{\{\alpha[\xi(q - q_{100})]^2 + 1\}^{\kappa}} \qquad (2)$$

with $\alpha = (2^{1/\kappa} - 1)/\pi^2$ and the positional correlation length $\xi = 2\pi/\mathrm{FWHM}$. The expression of the Pearson type VII profile reduces to a Lorentzian for $\kappa = 1$, to a SRL function for $\kappa = 0.5$, and to a Gaussian for $\kappa = \infty$ [25]. Eq. (2) has been convoluted with a Gaussian to account for the x-ray beam resolution [23]. A linear background contribution to intensity has also been subtracted, as shown by a dashed line in the corresponding figures. Experimentally, a SRL line shape fits with a good agreement ($\kappa = 0.56$) the Bragg reflection, including the peak tails, of the columnar phase, that features a hexatic structure. A Lorentzian distribution is found ($\kappa = 1.02$) for the smectic phase, that is consistent with the liquid order existing in the layers [Fig. 4(b)].

After the slow drying of a columnar sample during several weeks, a *crystalline phase* appears [Fig. 4(c)]. Contrary to the columnar phase, the crystalline phase exhibits translational order along the viruses, as shown by the presence of the (001) peak with $q_{001} = 0.075$ Å^{-1} [Fig. 4(c)]. This peak stems from *inter*-virus positional correlations between the fd coat proteins, which are helicoidally wrapped on a given virus following a fivefold rotation axis combined with a twofold screw axis [26]. By taking into account this C_5S_2 symmetry, the value of the (001) Bragg peak corresponds to the reported axial repeat distance between two coat proteins of 33 Å [26], which is close to $2/5 \times 2\pi/q_{001}$. Contrary to the columnar phase, the sharp high order reflections indicate both the existence of long-range hexagonal positional order [10], as expected for a crystal, and very little positional fluctuation. The interaxial distance for a hexagonal lattice between two particle cores $d = 4\pi/\sqrt{3}q_{100} = 61$ Å is found to be slightly smaller than the usual virus diameter D, as already observed in DNA suspensions [27]. It could be explained by some change in electronic contrast upon drying, that could be associated with some denaturation of the coat proteins. A fd concentration of 760 mg/ml has been measured in the crystalline phase, which corresponds to a volume fraction $\phi = 0.84$ with $D = 66$ Å, not far from the hexagonal close packing (CP) of rods with $\phi_{\mathrm{CP}} = \pi/2\sqrt{3} \simeq 0.91$. An analysis of the (100) diffraction peak has been performed for comparison with the smectic and columnar phases. The fit using Eq. (2) gives $\kappa = 1.08$, i.e., a Lorentzian profile [Fig. 4(d)], in agreement with the large width of the powder diffraction peak. Indeed, the diffraction peak broadening accounting for the crystallite finite size effect is empirically known to have a Lorentzian distribution [24]. This has to be distinguished from the so-called second-type disorder, first introduced by Guinier [28], which leads also to peak broadening. In this case, the peak width results from an inherent limited coherence of the crystalline lattice, as in the hexatic structure. Therefore, if the SRL diffraction peak profile demonstrates the hexatic feature of the columnar phase [19,22], it also rules out the peak broadening due to finite size effects. This is confirmed by the analysis involving the Laue-Scherrer relation [28], which relates the width of the Bragg peak to the translational correlation length, ξ. This coherence length is about $\xi \sim 0.1$ μm [Fig. 3(b)], i.e., much smaller than the typical domain size (~ 10 μm) observed by optical microscopy [Figs. 2(d) and 3(a)] or by SAXS [Fig. 2(a)].

While the existence of the columnar phase may be attributed to the rod flexibility [14], the occurrence of hexatic organization instead of long-range hexagonal ordering would stem from a geometrical frustration induced by the competition between long-range two-dimensional translational order and helical twist due the chirality of the virus [29]. Often this frustration is resolved via the introduction of topological defects as in the hexatic state, which appear to accommodate two competitive orders, as helical twist [17] or polydispersity [18] versus positional order. Several theoretical works on condensed states of biopolymers have pointed out the importance of the contribution of chirality, with the prediction of novel equilibrium structures [29,30], such as the tilt grain boundary phase or the "moiré" state. However, these models imply the existence of a hexatic pitch, which has never been experimentally demonstrated. That should stimulate fur-

ther theoretical and experimental investigations. Note that at higher virus density the rod packing entropy overcomes the helical twist for the stabilization of the crystalline phase.

In summary, structural characterizations by small angle x-ray scattering and optical microscopy on a model system of chiral semiflexible hard rods in the regime of high volume fractions have been achieved. The evidence of long-range sixfold orientational order and short-range translational order, mainly shown by a line shape analysis of the Bragg reflections, reveals a hexatic columnar structure. A second sixfold symmetry phase has been identified with increasing rod concentration: a hexagonal crystalline phase of viruses. The occurrence of these two novel condensed states opens the way towards the complete phase diagram determination of this model system of hard rods.

D. Durand and E. Belamie are acknowledged for the synchrotron beam time. We also thank F. Nallet for fruitful discussions.

*grelet@crpp-bordeaux.cnrs.fr

[1] A. Stroobants *et al.*, Phys. Rev. A **36**, 2929 (1987); G. J. Vroege *et al.*, Rep. Prog. Phys. **55**, 1241 (1992).

[2] F. C. Bawden *et al.*, Nature (London) **138**, 1051 (1936); F. Livolant *et al.*, Prog. Polym. Sci. **21**, 1115 (1996); B. J. Lemaire *et al.*, Phys. Rev. Lett. **93**, 267801 (2004); G. J. Vroege *et al.*, Adv. Mater. **18**, 2565 (2006).

[3] Z. Dogic and S. Fraden, in *Soft Matter*, edited by G. Gompper and M. Schick (Wiley-VCH, Weinheim, 2006), Vol. 2, and references therein.

[4] L. Onsager, Ann. N.Y. Acad. Sci. **51**, 627 (1949).

[5] D. Frenkel *et al.*, Nature (London) **332**, 822 (1988); J. A. C. Veerman *et al.*, Phys. Rev. A **43**, 4334 (1991); A. Stroobants, Phys. Rev. Lett. **69**, 2388 (1992).

[6] A. M. Bohle *et al.*, Phys. Rev. Lett. **76**, 1396 (1996); M. A. Bates *et al.*, J. Chem. Phys. **109**, 6193 (1998).

[7] The bacteriophage fd ($M_W = 1.64 \times 10^7$ g/mol) is formed by a single stranded DNA around which coat proteins are helicoidally wrapped. fd was grown using the XL1-Blue strain of *E. coli* as the host bacteria and purified following standard biological protocols [3]. To vary the ionic strength I, viruses were dialyzed against a 20 mM TRIS-HCl buffer at pH $= 8.2$ with an adjusted amount of NaCl. At this pH, the fd charge density is about 10 e/nm. The virus concentrations were measured using spectrophotometry with an absorption coefficient of 3.84 cm^2/mg at 269 nm. fd suspensions of different dilutions were placed in glass capillary tubes of diameter 1.5 mm.

[8] Z. Dogic *et al.*, Langmuir **16**, 7820 (2000); F. Tombolato *et al.*, Phys. Rev. Lett. **96**, 258302 (2006).

[9] Z. Dogic *et al.*, Phys. Rev. Lett. **78**, 2417 (1997); M. P. Lettinga *et al.*, Phys. Rev. Lett. **99**, 197802 (2007).

[10] Bragg reflections have been indexed according to the typical ratios of the scattering vector q: $1{:}\sqrt{3}{:}\sqrt{4}{:}\sqrt{7} : \ldots$ of a two-dimensional hexagonal lattice, corresponding, respectively, to the Miller indices $(hk\ell)$: (100), (110), (200), (210), ... with ℓ defined as the direction along the viruses.

[11] P. Oswald *et al.*, J. Phys. II (France) **6**, 281 (1996).

[12] F. Livolant *et al.*, J. Phys. (France) **47**, 1813 (1986).

[13] W. Pisula *et al.*, Adv. Funct. Mater. **15**, 893 (2005).

[14] R. Hentschke *et al.*, Phys. Rev. A **44**, 1148 (1991); J. V. Selinger *et al.*, Phys. Rev. A **43**, 2922 (1991); P. van der Schoot, J. Phys. II (France) **6**, 1557 (1996).

[15] J. M. Kosterlitz *et al.*, J. Phys. C **6**, 1181 (1973); B. I. Halperin *et al.*, Phys. Rev. Lett. **41**, 121 (1978).

[16] P. M. Chaikin and T. C. Lubensky, *Principles of Condensed Matter Physics* (Cambridge University Press, Cambridge, England, 1995).

[17] R. Podgornik *et al.*, Proc. Natl. Acad. Sci. U.S.A. **93**, 4261 (1996); H. H. Strey *et al.*, Phys. Rev. Lett. **84**, 3105 (2000).

[18] A. V. Petukhov *et al.*, Phys. Rev. Lett. **95**, 077801 (2005).

[19] S. C. Davey *et al.*, Phys. Rev. Lett. **53**, 2129 (1984); C. F. Chou *et al.*, Science **280**, 1424 (1998); C.-Y. Chao *et al.*, Phys. Rev. Lett. **93**, 247801 (2004).

[20] J. D. Brock *et al.*, Phys. Rev. Lett. **57**, 98 (1986); C. F. Chou *et al.*, Phys. Rev. Lett. **76**, 4556 (1996); G. E. Stein *et al.*, Phys. Rev. Lett. **98**, 086101 (2007).

[21] The beam of the anode x-ray generator (NanoStar- Bruker AXS) had a size of about 500 μm and a wavelength of $\lambda = 1.54$ Å. The instrumental resolution is given by the full width at half maximum (FWHM) of the direct beam, which was 0.0050 Å^{-1}.

[22] G. Aeppli *et al.*, Phys. Rev. Lett. **53**, 2133 (1984); I. R. Peterson *et al.*, Phys. Rev. Lett. **73**, 102 (1994); W. H. de Jeu *et al.*, Rev. Mod. Phys. **75**, 181 (2003).

[23] Synchrotron experiments were performed at the ESRF-ID02 beam line (Grenoble, France). The x-ray beam resolution function is approximated by a Gaussian distribution [24], with a vertical FWHM of 0.0021 Å^{-1} and a horizontal FWHM of 0.0033 Å^{-1}. The beam had a size of 150×300 μm^2 and a wavelength of $\lambda = 0.995$ Å. The sample-to-detector distance was varied from 1.2 to 2 m.

[24] T. H. de Keijser *et al.*, J. Appl. Crystallogr. **15**, 308 (1982); T. Ida *et al.*, J. Appl. Crystallogr. **33**, 1311 (2000); **34**, 144 (2001).

[25] M. M. Hall *et al.*, J. Appl. Crystallogr. **10**, 66 (1977); S. K. Gupta, J. Appl. Crystallogr. **31**, 474 (1998).

[26] L. C. Welsh *et al.*, Macromolecules **29**, 7075 (1996); D. A. Marvin *et al.*, J. Mol. Biol. **355**, 294 (2006).

[27] D. Durand *et al.*, J. Phys. II (France) **2**, 1769 (1992).

[28] A. Guinier, *X-ray Diffraction in Crystals, Imperfect Crystals, and Amorphous Bodies* (Dover, New York, 1994).

[29] R. D. Kamien *et al.*, Phys. Rev. Lett. **74**, 2499 (1995); **84**, 3109 (2000).

[30] V. Lorman *et al.*, Phys. Rev. Lett. **87**, 218101 (2001); M. J. Linehan, Phys. Rev. Lett. **88**, 065502 (2002); H. M. Harreis *et al.*, Phys. Rev. Lett. **89**, 018303 (2002); G. M. Grason *et al.*, Phys. Rev. Lett. **99**, 098101 (2007).